Effect of pressure on free-ion and crystal-field parameters of Pr^{3+} in $LOCl$ (L=La, Pr, Gd)

C. Bungenstock, Th. Tröster, and W. B. Holzapfel
FB 6 Physik, Universität Paderborn, 33095 Paderborn, Germany
(Received 15 March 2000)

Fluorescence and absorption spectra of Pr^{3+}:PrOCl (PrPr) were measured in the range from 11 500 cm^{-1} to 22 500 cm^{-1} under pressures up to 16 GPa. From these spectra, the pressure dependence of the energy-level scheme of the $4f^2$ configuration of Pr^{3+} could be partly derived. The effect of pressure on the free-ion parameters F^2, F^4, F^6, and ζ was determined and compared in detail with former results on Pr^{3+}:LaOCl (PrLa) and Pr^{3+}:GdOCl (PrGd). The observed shifts can be described by a combination of central-field and symmetry-restricted covalency in all cases. The variations of the crystal-field parameters are analyzed in the framework of the superposition model. Although specific features can be accounted for by this model, distinct deviations reveal the difficulties in applying this model to compounds with two different ligands.

I. INTRODUCTION

For many years the electronic structure of rare-earth ions in different host materials has been the subject of numerous investigations.[1,2] Due to the screening by outer shells, the energy-level scheme of the f configuration of a rare-earth ion in a crystal is very similar to the free-ion case. The crystal field, created by the surrounding ligands, only slightly affects the free-ion properties, leading to small shifts and splittings of the free-ion levels. Consequently, in optical measurements sharp lines are observed, corresponding to various electronic transitions between crystal-field levels of the f configuration.

Therefore, rare-earth ions serve as ideal candidates to study crystal-field effects. Additional application of high pressure has the advantage of continuously tuning the interatomic distances and therefore the crystal field, without changing other physical properties like the point symmetry of the rare-earth ion site or the chemical composition of the samples.

The $LOCl$ compounds crystallize in a tetragonal symmetry with space group $P4/nmm$. The rare-earth ions occupy one site with C_{4v} point symmetry. X-ray diffraction measurements on $LOCl$ proved the phase stability up to pressures above 50 GPa,[3] which is an important condition for the examination of crystal fields under high pressure and for the observation of large continuous changes of interatomic distances.

The experimental results for PrLa and PrGd have been presented already in recent publications.[4,5] The spectra of both samples were very similar, including the appearance of new lines under pressure that could not be assigned unambiguously. In this paper, the investigations were extended to PrPr mainly to verify whether the spectra show similar features, while local distortions, present in the other samples, can be excluded.

The knowledge of the variation of structural parameters is necessary to perform the superposition model[6,1] (SM) analysis of the crystal-field parameters. As mentioned before, for PrLa and PrGd, local distortions around the Pr^{3+} ion have to be taken into account. However, these local distortions can be estimated from a comparison of the optical and structural data of the doped and the pure sample under pressure.

Investigations of L^{3+}:$LaCl_3$ (L=Pr, Nd, U) under pressure[7–9] have shown that the SM indeed was able to describe the crystal-field variations with varying interatomic distances. In this paper the application of this model to $Pr^{3+}LOCl$ (PrLn, L=La, Pr, Gd) is presented. In comparison to $LaCl_3$, with one type of ligands only, the $LOCl$ host lattice represents a more difficult case, due to the two different ligands around the central Pr^{3+} ion. It is therefore a challenge for this work to check whether the SM and its assumptions are still valid.

II. EXPERIMENTAL DETAILS

The fluorescence measurements of PrPr presented here, were performed with the experimental setup described recently.[4] For the absorption spectra of PrPr, a halogen lamp was used.

The $LOCl$ samples were synthesized in the crystal-growth laboratory of the University of Paderborn. Starting materials were L_2O_3 with a fourfold excess of $LCl_3 7H_2O$, which was also used as fluxing agent. An appropriate amount of Pr_2O_3 was added to achieve a concentration of 1 mol % PrLn. All materials were mixed together in a crucible and dried for 12 h at 300 °C and subsequently heated up with 100 °C/h to 1000 °C in an Ar atmosphere. After reaction for 5 days, the furnace was slowly cooled down with a rate of 5 °C/h to 500 °C and subsequently with a rate of 50 °C to room temperature. The excess LCl_3 was dissolved in distilled water and the final single crystals in the shape of small ($\sim$50 μm ϕ) platelets were stored in dried Ar atmosphere.

III. OPTICAL SPECTRA OF Pr^{3+}:PrOCl

The measured spectra in the region from 11 000 cm^{-1} to 22 500 cm^{-1} consist of fluorescence transitions from the lowest level of $^3P_1$ and $^3P_0$ to ^3H_J (J=4,5,6) and ^3F_J (J=2,3,4). As in the case of PrLa and PrGd, the fluorescence originating from $^3P_0$ is much stronger than all other lines. However, in contrast to PrLa and PrGd, the fluorescence from the $^1D_2$ multiplet could not be observed neither by excitation with an argon-ion laser nor by resonant excitation with a dye laser. On the other hand, the $^3P_1$ fluo-

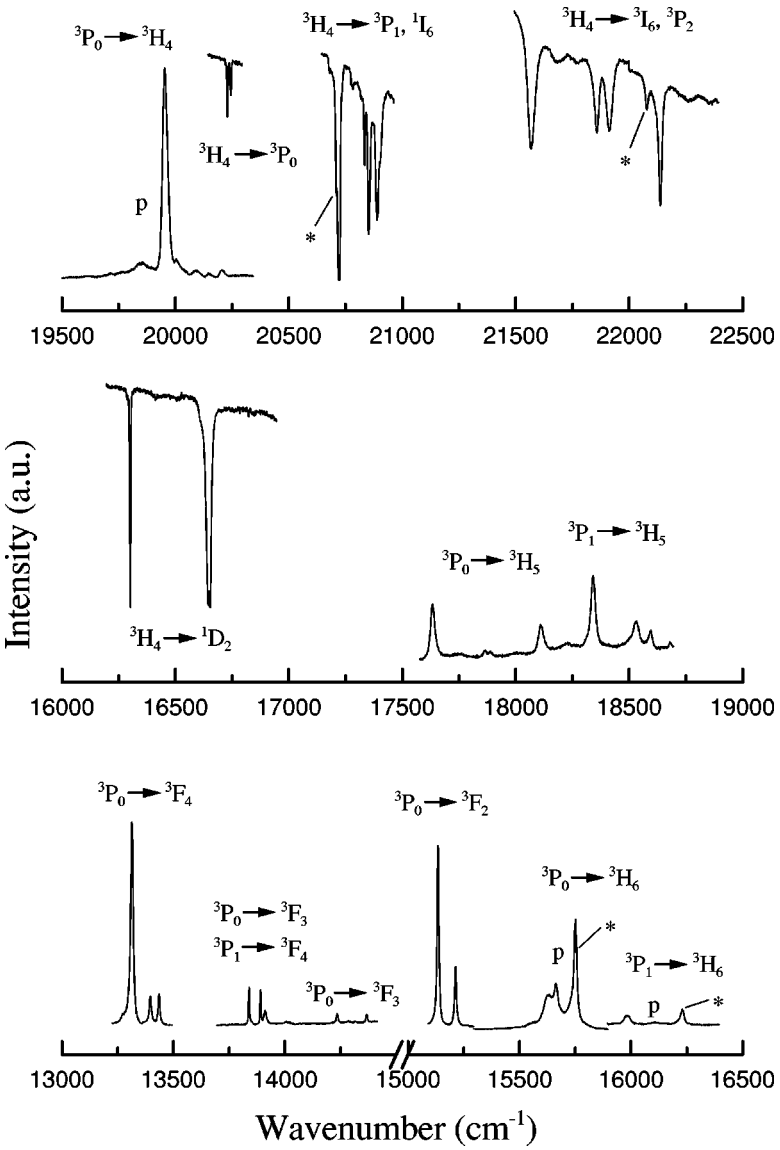

FIG. 1. Absorption and luminescence spectra of Pr^{3+}:PrOCl at ambient pressure and at 0.4 GPa (marked with *p*). All spectra were recorded at low temperatures (20 K). The asterisk denotes lines which could not be identified unambiguously.

rescence turned out to be significantly stronger. Thus, for PrPr also transitions from $^3P_1$ to $^3F_3$ and $^3F_4$ were observable over a wide range in pressure.

Due to the high Pr concentration it was possible also to observe absorption spectra from the ground state $^3H_4$ to $^1D_2$, $^3P_0$, $^3P_1$, $^1I_6$, and $^3P_2$. The spectra were taken at different temperatures varying between 2 K and 90 K. At 2 K only the lowest level of $^3H_4$ is occupied while at higher temperatures the increased population of excited levels of $^3H_4$ leads to additional lines. From the selection rules for electric-dipole transitions in C_{4v} point symmetry, it is possible to get information about the irreducible representation of the particular excited energy level that is involved in the absorption transition.

Figure 1 gives an overview of the observed fluorescence and absorption spectra of PrPr at ambient pressure and at 0.4 GPa (marked with *p*) in the range from 13 000 cm^{-1} to 22 500 cm^{-1}. The transitions from $^3P_0(A_1)$ and $^3P_1(A_2)$ to the ground state $^3H_4(E)$ were not observed, probably, because the emitted light was immediately reabsorbed within the crystal. To assign the different lines, various information like group-theoretical selection rules, similarities to the spectra of PrLa and PrGd, preliminary crystal-field calculations, observed pressure shifts, and temperature-dependent measurements (down to 2 K) were taken into account.

In addition, a former investigation of PrPr (Ref. 10) was helpful for comparison. Most levels found in the present investigation are identical with the former work, however, some distinct differences exist. One important deviation is the assignment of the ground state. In the present case the ground state was assigned to $^3H_4(E)$ whereas Antic-Fidancev *et al.*[10] assigned it to $^3H_4(A_1)$. The assignment in the present paper is based on various reasons. Most important here is a temperature-dependent measurement of the absorption spectra down to 2 K. At temperatures around 10 K only the two lowest components $^3H_4(E)$ and $^3H_4(A_1)$ are occupied. Thus, due to selection rules, only three transitions to $^3P_1$ are allowed (electric-dipole transitions). These transitions can indeed be observed in the region between 20 700 cm^{-1} and 21 000 cm^{-1}. The levels of $^3P_1$ in the present paper are in accordance with Ref. 10. Upon cooling down to 2 K, only the lowest component of $^3H_4$ remains occupied. If the ground state would be $^3H_4(A_1)$, only one line should remain, whereas in the case of $^3H_4(E)$ as the ground state, two lines should remain. Because the later was observed in our experiments, we assigned the ground state to

be $^3H_4(E)$. This is in agreement also with results for PrGd.[5]

In connection with this observation, an interesting point concerns the comparison of the ground level of all three samples. For PrGd the ground level is $^3H_4(E)$ and the first excited level $^3H_4(A_1)$. Under pressure a decrease of the E-A_1 splitting can be observed. In the case of PrPr at ambient pressure the situation is identical to PrGd. Under pressure, the E-A_1 splitting is also decreasing and even a crossing of the two levels can be observed at around 21 GPa. The level crossing could be identified clearly from temperature-dependent measurements and from the different sets of allowed transitions before and after the crossing. Finally, for PrLa the situation is identical to PrPr at pressures above 21 GPa, thus the ground level is $^3H_4(A_1)$ and the first excited level $^3H_4(E)$. Under pressure, this splitting simply increases. In fact, this observation is quite unexpected, because it is in contrast to the overall systematics just discussed. If only the pressure shifts of $^3H_4(A_1)$ and $^3H_4(E)$ are taken into account, exactly the opposite pressure systematics is found: PrGd $\overset{\text{pressure}}{\rightarrow}$ PrPr $\overset{\text{pressure}}{\rightarrow}$ PrLa.

Besides the lines which could be unambiguously identified, four unknown lines are observable, marked with an asterisk in Fig. 1. The origin of these lines is still not completely clear. However, their occurrence fits results for PrLa and PrGd, where extra lines could be observed also. Possible reasons for the existence of these lines were discussed in Ref. 4.

In view of the number of lines and intensity relations for the transitions between the crystal-field levels of two given multiplets, the fluorescence spectra of PrPr are very similar to those of PrLa and PrGd, not only at ambient conditions but also under pressure. It has been shown that the spectra of PrGd at ambient pressure corresponded to high-pressure spectra of PrLa.[5] Comparing the spectra of PrPr with PrLa it is found that the ambient pressure spectra of PrPr also correspond to the high-pressure spectra of PrLa, but at a much smaller pressure than in the case of PrGd. This series, PrLa $\overset{\text{pressure}}{\rightarrow}$ PrPr $\overset{\text{pressure}}{\rightarrow}$ PrGd, is also observable when the behavior of the unknown lines is studied. In the case of PrLa these extra lines are not observable at ambient pressure but appear only with increasing pressure. In the case of PrPr, already a few of these extra lines can be seen at ambient pressure, whereas in the case of PrGd all of them are observable from the beginning.

In total, the fluorescence and absorption spectra of PrPr allowed us to determine 32 energy levels at ambient pressure. These levels are listed in Table I. Under pressures up to 16 GPa, 26 of these energies remain observable.

TABLE I. Experimental and calculated energy levels of Pr^{3+}:PrOCl at ambient pressure.

Level		Energy (cm^{-1}) Exp.	Calc.	Level		Energy (cm^{-1}) Exp.	Calc.
$^3H_4$	E	0.0	29.7	$^3F_4$	A_1	6848.2	6828.1
	A_1	14.9	16.5		A_2	6872.5	6855.3
	B_1		108.6		B_2		6912.5
	E'	280.4	258.3		E'	6930.9	6957.2
	B_2		346.6		A_1'	6972.0	6992.1
	A_2		463.7				
	A_1'		493.8	$^1G_4$	B_1		9551.4
					E		9762.8
$^3H_5$	A_2	2126.9	2134.4		A_1		9854.1
	E	2133.3	2151.1		A_2		9902.4
	B_2		2178.5		B_2		9864.0
	B_1		2387.4		E'		10033.6
	E'	2380.8	2365.3		A_1'		10091.3
	A_1	2355.7	2334.7				
	A_2'		2398.1	$^1D_2$	B_2	16301.2	16292.8
	E''	2610.7	2580.8		B_1	16653.0	16661.5
					A_1		16692.9
$^3H_6$	A_1		4206.1		E		16759.3
	E	4249.9	4262.3				
	B_1		4339.1	$^3P_0$	A_1	20244.5	20240.8
	A_2		4503.9				
	E'		4496.0	$^3P_1$	A_2	20721.9	20728.7
	B_2		4554.5		E	20904.5	20898.5
	A_1'	4572.2	4575.6				
	E''		4602.2	$^1I_6$	A_1		20845.9
	B_1'		4846.7		E	20834.1	20834.7
	B_2'		4854.1		B_2	20853.3	20838.9
					B_1		21189.0
$^3F_2$	B_1		4946.2		E'		21238.8
	B_2		4996.3		A_2		21361.4
	E	5031.5	5040.4		A_1'		21451.1
	A_1	5110.2	5109.4		E''		21597.7
					B_2'	21568.8	21582.3
$^3F_3$	E	6353.8	6342.2		B_1'		21589.8
	B_1		6391.2				
	E'	6405.2	6413.1	$^3P_2$	B_2	21857.6	21851.0
	B_2		6410.6		B_1	21913.8	21916.0
	A_2	6487.5	6504.2		E	22114.5	22110.2
					A_1	22137.8	22145.0
$^3F_4$	B_1		6755.1				
	E	6809.5	6800.0	$^1S_0$	A_1		46148.5

IV. PARAMETER CALCULATIONS

Various physical interactions determine the energy-level scheme of the Pr^{3+} ion in a crystal. In general, the Hamiltonian used to calculate the energy levels is divided into a free-ion H_{FI} and a crystal-field part H_{CF}:

$$H = H_{FI} + H_{CF}.$$

The free-ion part can be written as:

$$H_{FI} = \sum_{k=0,2,4,6} f_k F^k + \zeta \sum_{i=1}^{N} s_i l_i + \alpha L(L+1) + \beta G(G_2) + \gamma G(R_7) + \sum_k P^k p_k + \sum_k M_k m_k.$$

A detailed discussion of this part can be found at various places in the literature.[11] For our purpose it is only important to recall that the free-ion interactions can be divided into radial and angular dependent parts. The angular dependence can be calculated exactly, whereas the radial parts are treated

TABLE II. Free-ion and crystal field parameter of Pr^{3+}:LOCl (L=La, Pr, Gd) at ambient pressure. Parameters marked with an asterisk were not varied.

	Pr^{3+}:LaOCl		Pr^{3+}:PrOCl		Pr^{3+}:GdOCl	
E_{ave}	9966		9947		9898	
F^2	67291	(59)	67288	(42)	67107	(47)
F^4	50141	(203)	49747	(177)	49896	(172)
F^6	32967	(113)	32926	(91)	32881	(102)
ζ	742	(2)	743	(2)	741	(2)
α	22	(*)	22	(*)	22	(*)
β	-700	(*)	-700	(*)	-700	(*)
γ	1422	(*)	1422	(*)	1422	(*)
M_0	1.76	(*)	1.76	(*)	1.76	(*)
P^2	275	(*)	275	(*)	275	(*)
B_0^2	-860	(26)	-670	(19)	-537	(23)
B_0^4	-411	(89)	-518	(78)	-581	(79)
B_4^4	914	(53)	803	(37)	788	(58)
B_0^6	696	(116)	1111	(136)	1150	(114)
B_4^6	-97	(112)	-89	(146)	-2	(116)
N	32		26		30	
σ	17.5		15.6		16.8	

as adjustable parameters. Their values are determined via least-squares fits of the calculated and experimental energy levels. The most important interactions are the Coulomb interactions, described by the Slater parameters F^k and the spin-orbit coupling, described by the spin-orbit coupling parameter ζ. The other parameters α, β, γ, M_k, and P^k represent minor corrections due to configuration and further magnetic interactions.

The general crystal-field Hamiltonian in the one-electron approximation is usually written as:

$$H_{CF}=\sum_{k,q} B_q^k C_q^{(k)}.$$

Analogous to the free-ion case, this Hamiltonian consists of radial parts, described by crystal-field parameters (CFP) B_q^k and angular parts $C_q^{(k)}$, which can be calculated exactly.

The determination of all these parameters via least-squares fits is possible only if sufficiently large data sets are available. Since this is not the case in the present paper, the values for some of the free-ion parameters were kept constant (under pressure). The results of the parameter fitting for PrLn at ambient pressure are summarized in Table II.

A. Free-ion parameters

As already mentioned, only the free-ion parameters F^k and ζ were treated as free parameters under pressure. The observed pressure dependence for all three samples is very similar. All the parameters show a decrease with increasing pressure, caused by the weakening of Coulomb and spin-orbit interactions, corresponding to the well-known nephelauxetic effect.[12] The relative decreases of these parameters are shown in Table III for PrLn under pressures of 16 GPa.

The main results can be summarized as follows:

(1) The relative decreases of the Slater parameters with increasing pressure are similar for all samples.

TABLE III. Relative decrease $\Delta=\Delta P/P$ (in percent) of the free-ion parameters F^k and ζ under pressures up to 16 GPa.

	Pr^{3+}:LaOCl	Pr^{3+}:PrOCl	Pr^{3+}:GdOCl
E_{ave}	-1.3 (1)	-1.5 (1)	-1.1 (1)
F^2	-1.5 (1)	-1.8 (1)	-1.7 (1)
F^4	-1.0 (1)	-0.9 (1)	-0.9 (1)
F^6	-0.5 (2)	-0.7 (2)	-0.3 (2)
ζ	-1.0 (1)	-1.0 (1)	-0.6 (2)
N	32	26	30
σ	17.5	15.6	16.8

(2) In all the cases the decreases of the Slater parameters can be ordered according to $\Delta F^2/F^2>\Delta F^4/F^4>\Delta F^6/F^6$.

(3) The relative decrease of the spin-orbit coupling parameter ζ is always smaller than the relative change of F^2 and comparable with the changes of F^4 and F^6.

These observations are similar to the former high-pressure results for L^{3+}:$LaCl_3$ (L=Pr, Nd) (Refs. 7 and 8) U^{3+}:$LaCl_3$ (Ref. 9) and Sm^{2+}:MFCl (M=Ba, Sr, Ca).[13]

B. Crystal-field parameters

The Hamiltonian H_{CF} for the crystal-field potential, introduced at the beginning of this section, is described in terms of a series expansion. Due to the C_{4v} point symmetry at the site of the Pr^{3+} ion in LOCl, however, only five terms of the series have to be taken into account:

$$H_{CF}=B_0^2C_0^{(2)}+B_0^4C_0^{(4)}+B_4^4C_4^{(4)}+B_0^6C_0^{(6)}+B_4^6C_4^{(6)}$$

and therefore only five adjustable configuration fraction percentage (CFP) B_q^k have to be varied in the fitting procedure.

The variation of the CFP with pressure for PrPr is shown in Fig. 2. Compared with the former results on PrLa (Ref. 4) and PrGd,[5] included in Fig. 2, a very similar behavior under pressure can be noticed. The common characteristics are the following:

(1) The absolute value of B_0^2 decreases with increasing pressure. The relative changes are between 33% and 38% in the range from 0 GPa to 16 GPa.

(2) Also B_0^4 decreases in its absolute value, but with a smaller relative change of about 15% to 18%.

(3) B_4^4 decreases also up to 16 GPa. However, in the case of PrPr the relative change of 30% is distinctly larger than for PrLa and PrGd, where it is only 15%.

(4) The B_0^6 parameter shows a strong increase and relative changes range between 50% and 66%.

(5) The decrease of B_4^6 is very similar for all three compounds. Nevertheless, this result must be taken with caution, because the statistical error of B_4^6 comes close to 100%.

The parameter fits for each sample had to be performed with different data sets. To avoid misinterpretations, these fits were also carried out with a reduced data set, which was the same for all three samples. This reduction of the data sets effected primarily the absolute values of the CFP B_q^k, especially of B_4^6, whereas the pressure dependence was only slightly changed. Therefore, the fits were carried out always with the largest possible data set for each sample to obtain parameters with smallest statistical errors.

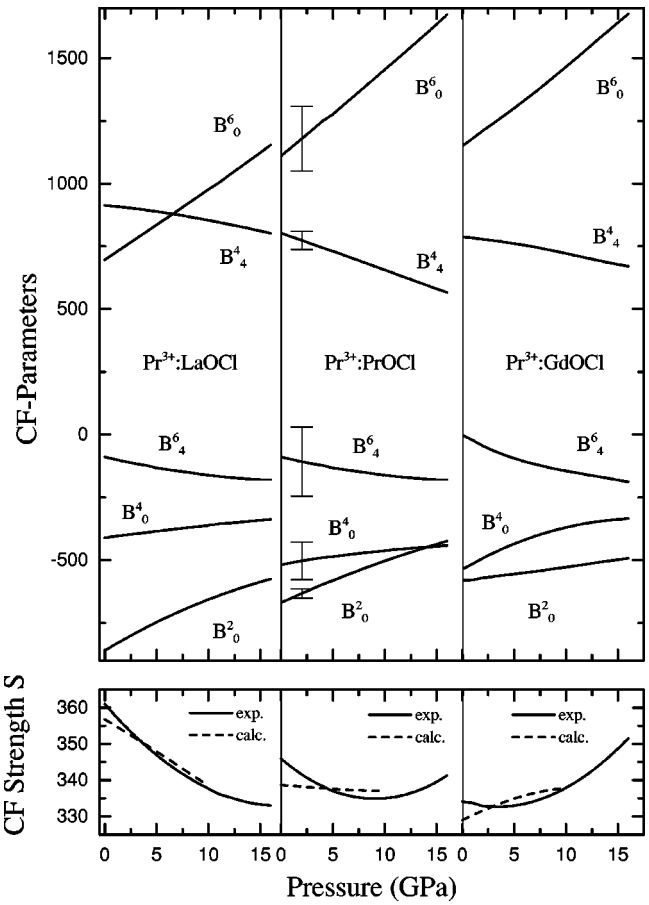

FIG. 2. Crystal-field parameters B_q^k $(kq=20,40,44,60,64)$ and crystal-field strength S for Pr^{3+}:LOCl under pressure.

From the CFP it is possible to calculate an overall crystal-field strength S according to the relation:[14]

$$S=\left\{\frac{1}{3}\sum_k \frac{1}{2k+1}\left[B_{k0}^2+2\sum_{m>0}(\Re B_{km}^2+\Im B_{km}^2)\right]\right\}^{1/2}. \tag{1}$$

This crystal-field strength and its pressure dependence for PrLa, PrPr, and PrGd is also shown in Fig. 2. In general, the observed changes with pressure fit to the ''pressure rule'' PrLa $\overset{\text{pressure}}{\rightarrow}$ PrPr $\overset{\text{pressure}}{\rightarrow}$ PrGd, which was discussed in Sec. III. However, the most astonishing feature here is an initial decrease of S for PrLa as well as for PrPr. In both samples a minimum can be observed, occuring at higher pressures for PrLa according to the ''pressure rule.'' Although, in general, increasing pressure is expected to increase the crystal-field strength due to decreasing distances between the f element and its ligands, a decrease in S can be explained also within the superposition model (see Sec. V B), if the geometrical factors decrease under pressure in such a way that they compensate the usual increase of the intrinsic parameters.

Another common feature for many of the rare-earth ions independent of the host material is the observation that some specific multiplets exist, which are not well described by the conventional crystal-field theory used here. A well-known example is the $^1D_2$ multiplet of the Pr^{3+} ion. This problem is observed also for the present samples. However, in addition to the $^1D_2$ multiplet, also the energy levels of $^3F_4$ are not well reproduced in LOCl. Different approaches tried to solve this general problem.[15–17] According to one of these suggestions[17,18] one can use a larger basis set in the calculation, which includes wave functions also for excited state configurations. The evaluation of the present data along this route is still in progress and may be completed soon.[19]

V. DISCUSSION

A. Free-ion models

Incorporation of a rare-earth ion into a crystalline environment results in a reduction of the free-ion energies. This so-called nephelauxetic effect is represented by a reduction of the free-ion parameters. The same effect continues to act under pressure, where the free-ion parameters show a further decrease.

The reduction of the free-ion parameters in a crystal has been attributed to different mechanisms. A well-known and sucessful model is based on covalency effects, where two alternative approaches can be distinguished.[20,12] First, within the ''screening model,'' the penetration of the ligand orbitals to the central ion orbitals with decreasing interatomic distances (corresponding to increasing pressure) results in a screening of the effective nuclear charge ''seen'' by the f electrons. Within this approach the free-ion parameters are related to the effective nuclear charge Z^* by:[21]

$$F^k \sim Z^* \quad \text{and} \quad \zeta \sim Z^{*3}.$$

For the small changes of the free-ion parameters observed under pressure, these relations imply:

$$\frac{\Delta F^k}{F^k}=\frac{\Delta Z^*}{Z^*} \quad \text{and} \quad \frac{\Delta \zeta}{\zeta}=3\frac{\Delta Z^*}{Z^*}.$$

Thus, the decrease of the Slater parameters should be three times weaker than the variation of the spin-orbit coupling parameter. However, the present results on PrLn (see Table III) reveal clearly that the reduction of the spin-orbit coupling parameter ζ is less or at the most equal to the reduction of the Slater parameters.

On the other hand, a second approach, called ''symmetry restricted covalency model,'' explains the decrease of the free-ion parameters by the increasing mixture of ligand and f orbitals with decreasing interatomic distances (i.e., increasing pressure). This mixture results in expanded molecular orbitals and thus in a reduction of the spin-orbit coupling and Coulomb interaction between the f electrons. In a first approximation, the Slater and spin-orbit coupling parameters are given by the expressions:

$$F^k \sim N^4 \quad \text{and} \quad \zeta \sim N^2,$$

whereby N represents a renormalization coefficient in terms of a sum including overlap intergrals and covalency parameters.[22] For small changes one obtains here:

$$\frac{\Delta F^k}{F^k}=4\frac{\Delta N}{N} \quad \text{and} \quad \frac{\Delta \zeta}{\zeta}=2\frac{\Delta N}{N}.$$

TABLE IV. Relative decrease of the free-ion parameters F^2 and ζ, the renormalization factor N and the effective nuclear charge Z^* for PrLn with values for three pressure intervals.

	Pr^{3+}:LaOCl			Pr^{3+}:PrOCl			Pr^{3+}:GdOCl		
Pressure(GPa)	0–5	5–10	10–15	0–5	5–10	10–15	0–5	5–10	10–15
$\frac{\Delta F^2}{F^2}(\%)$	-0.48	-0.48	-0.46	-0.56	-0.56	0.56	-0.58	-0.54	-0.48
$\frac{\Delta\zeta}{\zeta}(\%)$	-0.40	-0.32	-0.23	-0.33	-0.31	-0.31	-0.33	-0.20	-0.10
$CR=\frac{\Delta F^2}{F^2}\Big/\frac{\Delta\zeta}{\zeta}$	1.22	1.48	1.99	1.69	1.84	1.85	1.76	2.68	4.91
$\frac{\Delta N}{N}(\%)$	-0.11	-0.11	0.12	-0.14	-0.14	-0.14	-0.14	-0.14	-0.13
$\frac{\Delta Z^*}{Z^*}(\%)$	-0.06	-0.03	-0.0004	-0.02	-0.01	-0.01	-0.02	0.03	0.06

A useful quantity to distinguish both models is the covalency ratio CR:

$$CR=\frac{\Delta F^k}{F^k}\Big/\frac{\Delta\zeta}{\zeta}.$$

If only the screening model is responsible for the decrease of the free-ion parameters, CR should be equal to 1/3, if only the symmetry restricted model is important, CR should be equal to 2. An intermediate value between 1/3 and 2 would indicate that both types of contributions are essential.

Following the symmetry restricted covalency model, the decrease of the Slater parameters should be twice as strong as the variation of the spin-orbit coupling parameter. This behavior is indeed qualitatively observed in the present high-pressure experiments on PrLn as well as in former high-pressure studies[7,8,13,9] and in many cases, the experimental value CR fits close to this theoretical prediction (see Table IV). However, a closer inspection of all high-pressure studies shows that $CR=2$ is not always observed. The deviations are most significant for PrLa and U^{3+}:$LaCl_3$ (Ref. 9) in the low-pressure range up to 8 GPa. According to Table V one findsa particularly small value $CR=1.28$ for PrLa and the rather large value $CR=6.60$ for U^{3+}:$LaCl_3$.

Further deviations from this model are noticed for other rare-earth ions as for example Eu^{3+}. High-pressure experiments on Eu^{3+}:LaOCl (Ref. 13) and Eu^{3+}:GdOBr (Ref. 23) gave the values $CR=0.49$ and $CR=0.56$, respectively. These results indicate clearly, that the symmetry restricted covalency model is not appropriate to describe the situation for Eu^{3+} and also not for U^{3+}:$LaCl_3$.

In summary, none of the two approaches described provides a consistent frame to describe all the different f elements and their high-pressure behavior. Therefore, a reasonable way to account for all observations at the same time seems to require the application of both models simultanously. Using both models, the variation of the free-ion parameters can be expressed as follows:

$$\frac{\Delta F^k}{F^k}=\frac{\Delta Z^*}{Z^*}+4\frac{\Delta N}{N}$$

TABLE V. Relative decrease of the free-ion parameters F^2 and ζ, the renormalization factor N and the effective nuclear charge Z^* for Pr^{3+}, Nd^{3+}, Eu^{3+}, Sm^{2+}, and U^{3+} in different host lattices under pressures up to 8 GPa.

	$\frac{\Delta F^2}{F^2}(\%)$	$\frac{\Delta\zeta}{\zeta}(\%)$	$\frac{\Delta F^2}{F^2}\Big/\frac{\Delta\zeta}{\zeta}$	$\frac{\Delta N}{N}(\%)$	$\frac{\Delta Z^*}{Z^*}(\%)$	Ref.
Eu^{3+}:LaOCl	-0.31	-0.62	0.49	-0.03	-0.19	13
Eu^{3+}:GdOBr	-0.26	-0.45	0.56	-0.03	-0.13	23
Nd^{3+}:$LaCl_3$	-0.70	-0.40	1.75	-0.17	-0.02	8
Nd^{3+}:$NdCl_3$	-0.70	-0.30	2.33	-0.18	0.02	8
Pr^{3+}:LaOCl	-0.77	-0.60	1.28	-0.17	-0.09	4
Pr^{3+}:PrOCl	-0.90	-0.52	1.74	-0.21	-0.03	
Pr^{3+}:GdOCl	-0.91	-0.46	1.95	-0.23	-0.01	5
Pr^{3+}:$LaCl_3$	-1.00	-0.50	2.00	-0.25	0.00	8
Pr^{3+}:$PrCl_3$	-0.90	-0.30	3.00	-0.24	0.06	8
Sm^{2+}:MFCl	-1.17	-0.39	3.00	-0.31	0.08	13
U^{3+}:$LaCl_3$	-6.60	-1.00	6.60	-1.88	0.92	9

$$\frac{\Delta\zeta}{\zeta}=3\frac{\Delta Z^*}{Z^*}+2\frac{\Delta N}{N}.$$

From the experimental decreases ΔF^k and $\Delta\zeta$ under pressure, a simultaneous determination of $\Delta N/N$ as well as $\Delta Z^*/Z^*$ is possible. The results for this evaluation of the Slater parameter F^2 and the spin-orbit coupling parameter ζ are summarized in Table IV. To detect possible changes with increasing compression, the pressure range is divided into three sections. For F^4 and F^6, the values CR are slightly smaller, leading to smaller $\Delta N/N$ and larger $\Delta Z^*/Z^*$. However, the general trends in a comparison of different pressure ranges and different compounds do not change and all the conclusions drawn in the following discussion do not depend on the use of either F^2, F^4, or F^6. Thus, because of smaller statistical errors and because the absolute values and pressure dependencies of the Slater parameter F^2 in comparison to F^4 and F^6 are less affected by the choice of the data sets, the values for F^2 are used in the following discussion.

For all present PrLn samples, $\Delta N/N$ contributes the largest part to the decrease of F^2 and ζ. Only for PrLa in the low-pressure range, $\Delta Z^*/Z^*$ contributes significantly. This corresponds to a value for CR closer to 2 than to 1/3, which shows that the decrease of F^k and ζ is mainly caused by symmetry restricted covalency in the PrLn samples. It can be noticed also that the importance of the central-field covalency $\Delta Z^*/Z^*$ decreases with compression until its sign is reversed as for instance in PrGd around 5 GPa. This can be seen in Table IV as an approach of CR towards the value 2 and in the case of PrGd as an increase beyond the value 2 above 5 GPa. The sign reversal of $\Delta Z^*/Z^*$ for PrGd towards positive values above 5 GPa could reflect an antiscreening of the f electrons and will be discussed later in more detail.

So far the effects due to symmetry-restricted and central-field covalency were discussed for Pr^{3+} in the three isostructural LnOCl host materials only. Further information can be obtained from different host lattices and from other rare-earth ions under pressure. Some results are summarized in Table V. In all cases except for Eu^{3+} the decrease for F^2 is larger than for ζ. Thus, the symmetry-restricted covalency plays the dominant role. In the case of Eu^{3+}, on the contrary, the spin-orbit coupling parameter decrease more strongly than the Slater parameter, which leads to the conclusion that the central-field covalency is dominating here.

The Eu^{3+} ion is, compared to Pr^{3+}, Nd^{3+}, Sm^{2+}, and U^{3+}, the ion with the least expanded $4f$ wave function. Therefore, one may conclude that the symmetry-restricted covalency becomes increasingly more important when the wave function is expanded. This view is supported very strikingly by the data for U^{3+}, whose $5f$ wave function is much more expanded than the $4f$ wave functions of the other ions in Table V. For U^{3+}, the decrease of F^2 with respect to ζ is very large indicating that the classical central-field covalency does not play any significant role anymore, however the positive sign of $\Delta Z^*/Z^*$ can be interpreted as a result of a special ''antiscreening.''

These observations fit also to the high-pressure results in Table IV, which show an increasing influence of the symmetry restricted covalency with pressure as a consequence of the progressive expansion of the wave functions.

The different values for the same ion in different host crystals also confirm this general trend. For example, the sequence PrLa, PrPr, and PrGd of isostructural hosts corresponds to decreasing local distances around the Pr^{3+} ion and thus to an increasing internal pressure. The wave functions of the f electrons are thus expanding throughout this sequence, as shown by the decrease in the free-ion parameters at ambient pressure. Accordingly, the value CR increases from PrLa to PrPr and to PrGd and the same trend is observed also under pressure. Furthermore, identical results are obtained for the isostructural sequence Pr^{3+}:LCl_3 and Nd^{3+}:LCl_3.

An open question concerns the positive values for $\Delta Z^*/Z^*$ for PrGd above 5 GPa (see Table IV) and also for some other compounds listed in Table V. Positive values for this quantity are of course related to a value larger than two for the CR. A value larger than two means, that even the symmetry-restricted covalency model cannot account for the much stronger changes in the Slater parameters with respect to the spin-orbit coupling parameter. These unusually strong changes can be described in the combined model only if the effective nuclear charge increases.

It is not clear whether an increase in the effective nuclear charge is reasonable. In principle, such an increase could be explained by an increased covalency between the inner shell electrons and the ligands, leading to a charge transfer from inner shells to the ligands and thus to an increase of the effective nuclear charge Z^* for the f electrons. This effect could be called ''antiscreening.'' On the other hand, if the effective nuclear charge does not change at all at strong compression, it would mean that the symmetry-restricted model cannot describe the situation at strong compression or for strongly expanded wave functions.

In any case, the analysis of the free-ion parameters for PrLn and also for other rare-earth ions in different host materials under pressure leads to a coherent picture. The nephelauxetic effect can be described by a combination of central-field and symmetry-restricted covalency and depends on the expansion of the f electron wave functions. Only at very high pressures or in the case of strongly expanded wave functions the results from this model are not completely clear.

B. Superposition model

The CFP discussed in Sec. IV B, still contains all the structural information about the local environment. Therefore, at this stage a direct comparison of CFP values with results from other hosts is not reasonable. A transferable set of parameters can be generated however, if the structural information is extracted as illustrated by the SM, which reduces the CFP to a set of intrinsic parameters, depending on interatomic distances and the type of ligands only.

In fact, this model is based on the assumption that the crystal-field components are additive and builtup from the contributions of the individual ligands. Interactions between the ligands are ignored thereby. In general, only the nearest neighbors are taken into account. Within the SM, the phenomenological CFP B_q^k can be expressed by intrinsic parameters $\overline{B}_k$ and geometrical factors K_{kq} as follows:[24]

TABLE VI. Local distortions of distances ΔR_{Ln} (pm) and angles $\Delta\theta_{Ln}$ (°) around the central ion with respect to the structural parameters of the host. The pressure dependence for each quantity is given by $\Delta X = \Delta X_0 + \Delta X_0' p$ (GPa).

	LaOCl		GdOCl	
	ΔX_0 (pm)	$\Delta X_0'$ (pm/GPa)	ΔX_0 (pm)	$\Delta X_0'$ (pm/GPa)
ΔR_{Cl}	-3.5	0.29	4.4	0.16
$\Delta R_{\mathrm{Cl}}'$	-1.7	0.35	2.0	0.09
ΔR_{O}	-3.3	0.07	6.0	0.00
	ΔX_0 (°)	$\Delta X_0'$ (°/GPa)	ΔX_0 (°)	$\Delta X_0'$ (°/GPa)
$\Delta\theta_{\mathrm{Cl}}$	-0.4	0.03	1.0	0.01
$\Delta\theta_{\mathrm{O}}$	0.0	-0.04	0.4	-0.04

$$B_q^k(r) = \sum_j \overline{B}_k(r, R_j) K_{kq}(\vartheta_j, \varphi_j).$$

The intrinsic parameters $\overline{B}_k$ should depend then only on the kind of the ligand j at the distance R_j. Because the SM does not make any assumptions about the nature of the crystal field, its intrinsic parameters can account for all the interactions that occur between an f electron of the central ion and one ligand. The geometrical factors K_{kq} only depend on the angular coordinates ϑ_j, φ_j of the ligands. The effect of pressure on these geometrical factors can be calculated directly if the structural changes under pressure are known.

The Pr^{3+} ion in LOCl is surrounded by four O^{2-} ions located in a plane below the central ion at the distance R_{O}, four Cl^- ions in a plane above the central ion at the distance R_{CL}, and one Cl^- ion above the Cl^- plane at the distance $R_{\mathrm{CL}'}$. The sum of the contributions from these ligands give for the crystal-field parameters B_q^k with $k = 2,4,6$ $(k \geqslant q)$ the forms:

$$B_0^k = 4\overline{B}_k^{\mathrm{O}}(R_{\mathrm{O}}) K_{k0}^O + 4\overline{B}_k^{\mathrm{Cl}}(R_{\mathrm{Cl}}) K_{k0}^{\mathrm{Cl}} + \overline{B}_k^{\mathrm{Cl}}(R_{\mathrm{Cl}'}) K_{k0}^{\mathrm{Cl}'}, \quad (2)$$

$$B_4^k = 4\overline{B}_k^{\mathrm{O}}(R_{\mathrm{O}}) K_{k4}^O + 4\overline{B}_k^{\mathrm{Cl}}(R_{\mathrm{Cl}}) K_{k4}^{\mathrm{Cl}}. \quad (3)$$

For every ligand L (L = Cl or O) a set of three intrinsic parameters $\overline{B}_k^L$ exists. For the distance dependence of the intrinsic parameters $\overline{B}_k^L$ a simple power law is commonly used:

$$\overline{B}_k^L(R_L) = \overline{B}_k^L(R_L^0)\left(\frac{R_L^0}{R_L}\right)^{t_k^L}.$$

The quantities $\overline{B}_k^L(R_L^0)$ and t_k^L are treated as adjustable parameters, R_L^0 is a reference distance that can be chosen arbitrarily. The intrinsic fit parameters $\overline{B}_k^L(R_0)$ and the distance dependencies, represented by the exponents t_k^L, can be deduced from the CFP only if the variations of the bond angles and distances between the central Pr^{3+} ion and its ligands in LOCl under pressure are well known.

From x-ray diffraction and extended x-ray-absorption fine structure measurements on LOCl (L = La, Pr, Gd) under pressure, it was at first possible to determine the distances and angles around the L ion in the pure samples.[3] However, for the doped samples PrLa and PrGd, the local distortions around the Pr^{3+} ion must be taken into account also.

One method to estimate these distortions is based on the assumption that the energies of the crystal-field levels of the Pr^{3+} ion are mainly determined by the nearest neighbors and their geometrical arrangement. This means, that all the energy levels of Pr^{3+} in two different isostructural hosts are only equal, if the nearest neighbor distances and angles are also the same. According to this consideration, the spectra of PrLa and PrGd were compared with those from PrPr, which is used as the reference material without local distortions. The exact procedure to determine the local distortions with this method were described in detail previously.[7]

Based on this method, Table VI gives the local distortions for the Pr^{3+} ion in LaOCl and GdOCl. The final results for the intrinsic fit parameters $\overline{B}_k^L(R_0)$, taking into account the local distortions in the case of PrLa and PrGd, are shown in Table VII. The analysis was carried out for the pressure range up to 10 GPa, for which structural data are available for all host materials.[3] For the present PrLn samples, the local distortions led only to minor changes in the intrinsic fit parameters.

As mentioned before, changes in the geometrical factors can account for a decrease in the crystal-field strength, even though the intrinsic parameters are steadily increasing with decreasing distances. The decrease in crystal-field strength may be either due to decreasing values of the geometrical factors themselves or to changing contributions from different ligands with opposite signs of the factors. This is exactly what can be observed in the present paper. Although the intrinsic parameters increase with decreasing distances (see Table VII), the calculated crystal-field strength, especially for PrLa, turns out to decrease under pressure. This is demonstrated in Fig. 2, where the calculated crystal-field strength has been added to the figure.

TABLE VII. Intrinsic crystal-field parameters (in cm^{-1}) for PrLa, PrPr, and PrGd. ΔB_q^k represent special shifts for B_0^4 and B_4^4 explained in the text.

$R_0^{\mathrm{Cl}} = 316$ pm	$\overline{B}_2^{Cl}(R_0)$	t_2^{Cl}	$\overline{B}_4^{Cl}(R_0)$	t_4^{Cl}	$\overline{B}_6^{Cl}(R_0)$	t_6^{Cl}	ΔB_0^4	ΔB_4^4
Pr^{3+}:LaOCl	906(26)	5(2)	172(25)	10(2)	181(43)	11(2)	351	327
Pr^{3+}:PrOCl	908(36)	5(2)	189(28)	13(2)	308(28)	(2)	205	226
Pr^{3+}:GdOCl	898(84)	5(2)	163(31)	12(2)	298(43)	9(2)	150	190
$R_0^{\mathrm{O}} = 235$ pm	$\overline{B}_2^{O}(R_0)$	t_2^O	$\overline{B}_4^{Cl}(R_0)$	t_4^O	$\overline{B}_6^{Cl}(R_0)$	t_6^O		
Pr^{3+}:LaOCl	2229(177)	-1(1)	722(69)	8(3)	214(24)	12(2)		
Pr^{3+}:PrOCl	1819(189)	-1(2)	705(47)	7(3)	272(50)	10(2)		
Pr^{3+}:GdOCl	1607(70)	-1(2)	693(23)	9(2)	236(22)	11(3)		

The intrinsic fit parameters $\overline{B}_6^{\mathrm{Cl}}(R_0)$, t_6^{Cl}, $\overline{B}_6^{\mathrm{O}}(R_0)$, and t_6^{O} were determined from a least-squares fit of the calculated CFP B_0^6 and B_4^6 under pressure. However, in the cases of PrLa and PrGd, the parameter B_4^6 could be described only if a negative exponent t_6^{O} was used. So far, neither experimental studies nor *ab initio* calculations gave any hints for negative exponents for $k=6$ intrinsic parameters. Since the B_4^6 parameters contain large statistical errors, it appeared to be more reasonable therefore to exclude B_4^6 from the determination of $\overline{B}_6^L$ parameters for PrLa and PrGd. These results are shown in Table VII.

With this procedure, the absolute values calculated for B_4^6 of PrLa and PrGd are deviating from the experimental values, however, the pressure dependencies are reproduced quite well. This observation further justifies the decision to exclude B_4^6 from the determination of the intrinsic fit parameters also from the point of view that the statistical uncertainties effect the absolute values of the crystal-field parameters more than the pressure dependence.

Within the estimated uncertainties, Table VII shows that a common set of intrinsic fit parameters with $k=6$ can be found to describe all samples studied here. One remarkable difference is only observed in the case of $\overline{B}_6^{\mathrm{Cl}}(R_0)$ for PrLa. However, this difference is caused here only by the use of different data sets in the determination of the CFP B_q^6. If the CFP determined from identical data sets for all three samples are used, very similar values of $\overline{B}_6^{\mathrm{Cl}}(R_0)\approx 250(50)\ \mathrm{cm}^{-1}$ are obtained for all PrLn samples.

More serious difficulties were encountered in the case of the intrinsic parameters $\overline{B}_4^L$. In this case, four intrinsic fit parameters have to be determined, two absolute values $\overline{B}_4^{\mathrm{Cl}}(R_0)$ and $\overline{B}_4^{\mathrm{O}}(R_0)$ and two distance dependencies t_4^{Cl} and t_4^{O}. In principle, the determination of these parameters is always possible because four experimental quantities exist as well, namely, the absolute values of B_0^4 and B_4^4 and their respective pressure dependencies. However, a simple least-squares fit of the intrinsic parameters led to absurd results here. For example, for PrLa both exponents t_4^{Cl} and t_4^{O} turned out to be negative. Forcing the exponents to some positive values, it was found that in none of the samples it was possible to derive the absolute values of the $k=4$ CFP with reasonable error limits.

Reasonable and consistent values for the intrinsic parameters $\overline{B}_4^L$ could be obtained only by the introduction of two further parameters ΔB_0^4 and ΔB_4^4 in the fitting procedure. These parameters represent pressure independent constants, added to the calculated CFP. The values for these quantities are also listed in Table VII.

These necessary corrections for the CFP B_0^4 and B_4^4 cannot be explained by uncertainties in the absolute values due to the limited energy level data sets, but clearly indicate limitations of the SM itself in the case of the LOCl compounds. The problem seems to be related mainly to the absolute values calculated for B_0^4 and B_4^4, whereas the pressure dependencies are described well, when the constant corrections were taken into account. This suggests that a part of the CFP consist of interactions which are not included in the SM, like long-range electrostatic[25] or ligand-ligand interactions.[26] Especially in the case of long-range electrostatic interactions it was shown, that for example in the case of Er^{3+}:$LiErF_4$, distinct changes of the CFP of up to 30% can be expected,[25] which would explain the large corrections necessary here.

For $k=2$ only one CFP B_0^2 is available to determine the intrinsic parameters $\overline{B}_2^L$. In addition, from *ab initio* calculations[26] it is known, that especially this parameter is strongly effected by long-range electrostatic interactions in contrast to the assumptions of the SM. Despite these limitations, values for $\overline{B}_2^L(R_0)$ and t_2^L were determined and included in Table VII.

A closer inspection of Table VII reveals that the intrinsic fit parameters obtained for the chloride ligands are very similar for all PrLn samples studied so far. It is interesting to note that *ab initio* calculations for the $\overline{B}_2^{\mathrm{Cl}}$ parameter yield similar results as the experiment.

However, in the case of the oxygen ligands two interesting features can be noticed. First, one finds negative values for the exponent t_2^{O} and second, the absolute value of the intrinsic fit parameter $\overline{B}_2^{\mathrm{O}}(R_0)$ is unusually large and varies strongly from one compound to the other.

In fact, the negative value for t_2^{O} is reproduced by the *ab initio* calculations.[27] However, the experimental value for the $\overline{B}_2^{\mathrm{O}}(R_0)$ parameter is much larger than the calculated value. This discrepancy could be related to long-range electrostatic interactions.

In the case of $k=4$ and $k=6$, in total four quantities $\overline{B}_k^{\mathrm{Cl}}(R_0)$, $\overline{B}_k^{\mathrm{O}}(R_0)$, t_k^{Cl}, and t_k^{O} for the two intrinsic parameters for chloride and oxygen ligands had to be determined. Indeed, four experimental quantities were measured, the absolute values of B_0^k and B_4^k at ambient conditions and their pressure dependencies (see explanations above). However, in the case of the $k=2$ intrinsic parameters, only one CFP B_0^2 and its pressure dependence is available. Therefore, the number of experimental quantities is smaller than the number of intrinsic fit parameters to be determined. From this point of view, it is easy to find intrinsic fit parameters that exactly describe the single CFP B_0^2. Therefore, these parameters can absorb also effects that are not included in the SM, with the consequence, that the experimental intrinsic parameters can deviate strongly from the *ab initio* calculated values.

If the reason for the constant corrections in the case of $k=4$ parameters is assumed to lie in long-range electrostatic interactions,[25] the contribution to the CFP B_0^2 should be even more pronounced. However, these contributions may not result in difficulties with the single B_0^2 parameter, but may lead only to unusually large values for the intrinsic fit parameters. Therefore, it may be argued that the much larger values of the intrinsic fit parameters $\overline{B}_2^{\mathrm{O}}(R_0)$, compared to the *ab initio* calculations, are due to omitted long-range electrostatic interactions. In this context, also the behavior of ΔB_q^4 and $\overline{B}_2^{O}(R_0)$ in the sequence PrLa-PrPr-PrGd should be mentioned, which points to a common reason for these discrepancies.

To compare the results for PrLn of the present paper with other experimental data found in the literature, Table VIII summarizes intrinsic fit parameters for various rare-earth ions in different host materials. Due to the special difficulties

TABLE VIII. Intrinsic crystal-field parameters of various rare-earth ions in different host materials. Bold numbers indicate data where the values with the given statistical errors deviate significantly from the average values.

$R_0^{Cl}=316$ pm	$\overline{B_4^{Cl}}(R_0)$	t_4^{Cl}	$\overline{B_6^{Cl}}(R_0)$	t_6^{Cl}	Ref.
Pr^{3+}:*L*OCl	175(28)	**12**(2)	**292**(38)	10(2)	
Pr^{3+}:$LaCl_3$	204(33)	5(4)	161(42)	7(2)	8
[a]Pr^{3+}:$Cs_2NaPrCl_6$	176(35)	8(4)	**112**(22)	12(6)	28
Nd^{3+}:$LaCl_3$	149(49)	4(2)	187(46)	6(2)	8
[a]Eu^{3+}:$LaCl_3$	191(–)	6(1)	230(–)	6(1)	29
Average	179(17)	7(2)	196(19)	8(2)	
$R_0^{O}=235$ pm	$\overline{B_4^{O}}(R_0)$	t_4^{O}	$\overline{B_6^{O}}(R_0)$	t_6^{O}	Ref.
Pr^{3+}:LnOCl	**706**(46)	8(2)	**241**(32)	11(2)	
Nd^{3+}:Nd_2O_3	827(129)	6(-)	440(43)	6(-)	2
[a]Eu^{3+}:La_2O_3	1219(244)	10(5)	324(65)	11(6)	29
[a]Eu^{3+}:La_2O_2S	956(192)	10(5)	414(83)	11(6)	29
[a]Eu^{3+}:$LaAlO_3$	1042(208)	10(5)	**1114**(223)	11(6)	29
Average	950(80)	9(3)	[b]355(30)	10(3)	

[a]Without local distortions.

[b]$\overline{B_6^{O}}(R_0)$ for Eu^{3+}:$LaAlO_3$ was not taken into account.

for the $k=2$ parameters just mentioned above, $k=2$ values are rarely given in the literature and thus only $k=4$ and $k=6$ parameters are listed. As already mentioned, the intrinsic parameters depend only on the type of ligand and its distance to the *f* element. Thus, in a first approximation, in the scope of this model, different rare-earth ions can be directly compared and should lead to similar parameters. For PrLn an average value of all three samples is given in Table VIII.

In the case of Pr^{3+}:Cs_2NaYCl_6 as well as for all samples with the Eu^{3+} ion, local distortion around the doped ion were not taken into account. However, according to previous investigations on Nd^{3+}:$LaCl_3$,[8] L^{2+}:MF_2 (M=Ca, Sr, Ba) (Ref. 28) and Sm^{2+}:*M*FCl (M=Ba, Sr) (Ref. 13) the local distortions may result in changes of up to 50% for the exponents and up to 20% for the $\overline{B_k^l}(R_0)$. These uncertainties were used as estimated errors given in the table for the compounds without considering local distortions.

The table also gives average values for the different intrinsic parameters. In general, only a few values deviate significantly from these average values, as indicated by bold numbers. This observation indicates that the SM can be used as a common frame to analyze the CFP. However, the deviations have to be taken serious and in fact clearly show the limitations and difficulties that may arise within this model.

In detail, the following deviations appear to be significant: (1) in the case of PrLn the chloride values t_4^{Cl} and $\overline{B_6^{Cl}}(R_0)$ are both unusually large, whereas the oxygen values $\overline{B_4^{O}}(R_0)$ and $\overline{B_6^{O}}(R_0)$ are both unusually small, (2) for Pr^{3+}:Cs_2NaYCl_6 the parameter $\overline{B_6^{Cl}}(R_0)$ is unusually small, and finally (3) for Eu^{3+}:$LaAlO_3$ the parameter $\overline{B_6^{Cl}}(R_0)$ is unusually large.

In case (2), the intrinsic fit parameters were determined from a comparison of the CFP for Pr^{3+}:Cs_2NaYCl_6 with that for Pr^{3+}:$LaCl_3$. In both compounds local distortions were not taken into account. Thus, it cannot be ruled out that the estimated error of 20%, which originates from experiences with high-pressure studies, actually is much larger. Therefore, from this deviation alone one cannot infer that the assumptions of the SM are invalid. A similar problem exists for case (3). Both cases represent singular exceptions from the general trend and may be explained by difficulties arising from different data sets or local distortions.

More seriously are the deviations of case (1). One possible explanation may be related to long-range electrostatic interactions, which cannot be accounted for by the SM.[25] However, at least for the $k=6$ parameters these interactions should have a negligible influence, which rules out this interaction to explain all differences.

The present paper is the only case in Table VIII that provides data from two different ligands around the central ion. From this point of view, it is not clear whether further problems for the application of the SM arise in this case due to omission of ligand-ligand interactions. In a study on Sm^{2+} in solids with chloride and fluoride ligands[26] it was found that ligand-ligand interactions may lead to distinct changes of the intrinsic parameters if two different ligands are present. In that case, the intrinsic parameters of the chloride ions increased and simultaneously, the fluoride intrinsic parameters decreased. In this sense, ligand-ligand interactions could be responsible for increased chloride and decreased fluoride parameters, which would explain also the deviations found in the present PrLn samples.

In any case, present high-pressure results can be explained only if one releases some of the assumptions typical for the SM. Thus, the high-pressure studies reveal clearly limitations of the SM, possibly caused by long-range electrostatic or ligand-ligand interactions.

VI. CONCLUSIONS

The comparison of the present energy level shifts for PrPr under pressure with former results on PrLa and PrGd shows, that the samples can be ordered in the pressure series PrLa $\xrightarrow{\text{pressure}}$ PrPr $\xrightarrow{\text{pressure}}$ PrGd. The free-ion and crystal-field parameters derived from the energy-level shifts fit to this ''pressure rule.''

The observed reduction of the free-ion parameters F^k and ζ correspond to the Nephelauxetic effect and were explained by a combination of the central-field and symmetry-restricted covalency model. Analyzing the high-pressure results as well as literature data at ambient pressure, a general trend for the relative importance of these two models could be derived. According to this, the symmetry-restricted covalency becomes more and more important the larger the expansion of the *f* electron wave function is.

The crystal-field parameters were analyzed in terms of the SM. Although this model provides a consistent frame to describe some ambient as well as some high-pressure results, certain deviations are noticed. Especially the present high-pressure data for hosts with two different ligands require modifications of the SM, possibly related to long-range electrostatic or ligand-ligand interactions that are not included in the SM.

ACKNOWLEDGMENTS

This work was supported by the Deutsche Forschungsgemeinschaft (DFG) under Grant No. HO 486/21.

[1] D. J. Newman, Adv. Phys. **20**, 197 (1971).
[2] D. Garcia and M. Faucher, in *Handbook on the Physics and Chemistry of Rare Earths*, edited by K. A. Gschneidner, Jr. and L. Eyring (North Holland, Amsterdam, 1995), Vol. 21, Chap. 144.
[3] C. Bungenstock, G. Reiß, F. Nessel, H. Giefers, G. Nowitzke, G. Wortmann, W. B. Holzapfel, J. Haines, and J. M. Leger, J. Phys.: Condens. Matter (to be published).
[4] C. Bungenstock, Th. Tröster, W. B. Holzapfel, R. Bini, L. Ulivi, and S. Cavalieri, J. Phys.: Condens. Matter **10**, 9329 (1998).
[5] C. Bungenstock, Th. Tröster, W. B. Holzapfel, L. Fini, and M. Santoro, J. Phys.: Condens. Matter (to be published).
[6] M. I. Bradbury and D. J. Newman, Chem. Phys. Lett. **1**, 44 (1967).
[7] T. Gregorian, H. d'Amour-Sturm, and W. B. Holzapfel, Phys. Rev. B **39**, 12 497 (1989).
[8] Th. Tröster, T. Gregorian, and W. B. Holzapfel, Phys. Rev. B **48**, 2960 (1993).
[9] T. Tröster and W. B. Holzapfel, Phys. Rev. B **51**, 14 892 (1995).
[10] E. Antic-Fidancev, M. Lemaitre-Blaise, P. Porcher, and J. Hölsä, J. Chem. Soc., Faraday Trans. **87**, 3625 (1991).
[11] W. T. Carnall, G. L. Goodman, K. Rajnak, and R. S. Rana, J. Chem. Phys. **90**, 3443 (1989).
[12] R. Reisfeld and C. K. Jorgensen, *Lasers and Exited States of Rare Earths* (Springer-Verlag, Berlin, 1977).
[13] Y. Shen and W. B. Holzapfel, Phys. Rev. B **52**, 12 618 (1995).
[14] N. C. Chang, J. B. Gruber, R. P. Leavitt, and C. A. Morrison, J. Chem. Phys. **76**, 3877 (1982).
[15] M. F. Reid, J. Chem. Phys. **87**, 2875 (1987).
[16] G. W. Burdick and F. S. Richardson, J. Alloys Compd. **275-277**, 379 (1998).
[17] D. Garcia and M. D. Faucher, J. Chem. Phys. **90**, 5280 (1989).
[18] D. Garcia and M. D. Faucher, J. Chem. Phys. **91**, 7461 (1989).
[19] Th. Tröster, C. Bungenstock, and W. B. Holzapfel (unpublished).
[20] C. K. Jorgensen, *Modern Aspects of Ligand Field Theory* (North-Holland, Amsterdam, 1971).
[21] Z. B. Goldschmidt, in *Handbook of the Physics and Chemistry of Rare Earths*, edited by K. A. Gschneidner, Jr. and L. Eyring (North-Holland, Amsterdam, 1978), Vol. 1, Chap. 1.
[22] D. J. Newman, B. Ng, and Y. M. Poon, J. Phys. C **17**, 5577 (1984).
[23] Y. Chi, H. Li, S. Liu, X. Zhao, and L. Wang, J. Alloys Compd. **256**, 1 (1997).
[24] D. J. Newman and B. Ng, Rep. Prog. Phys. **52**, 699 (1989).
[25] B. Z. Malkin, in *Spectroscopy of Solids Containing Rare Earth Ions*, edited by A. A. Kaplyanskii and R. M. Macfarlane (North-Holland, Amsterdam, 1987), p. 13.
[26] Y. R. Shen and K. L. Bray, Phys. Rev. B **58**, 5305 (1998).
[27] Y. Shen (private communication).
[28] D. J. Newman, Aust. J. Phys. **31**, 79 (1978).
[29] C. Linares and A. Louat, J. Physique **36**, 49 (1975).